Physics of the Solid State, 2023, Vol. 65, No. 1

03,04,10

Electronic structure and lattice dynamics of Be_2NA ($A = $ F, Cl, Br, I) with an antichalcopyrite structure

© *A.B. Gordienko*[1], *Yu.M. Basalaev*[2], *V.S. Timofeev*[1]

[1] Kemerovo State University,
Kemerovo, Russia
[2] Kemerovo State Medical University,
Kemerovo, Russia
E-mail: gordi@kemsu.ru

Received October 10, 2022
Revised October 10, 2022
Accepted October 11, 2022

The new group of compounds with an antichalcopyrite structure and being isocationic series of Be_2NA ($A = $ F, Cl, Br, I) is studied within the local approximation of density functional theory. The results of the calculations performed include the basic parameters of crystal structure characteristics of electronic structure, lattice dynamics and chemical bonding based on maps of electronic density and electron localization function, which exhibit a well-pronounced dependence on the atomic number of the halogen atoms.

Keywords: band structure, chemical bonding, phonon spectra.

DOI: 10.21883/PSS.2023.01.54977.495

1. Introduction

Compounds containing beryllium in combination with nitrogen, fluorine, chlorine, bromine and iodine atoms are of practical interest as materials with a wide band gap and semiconductor properties. At the same time, they can also be considered as a basis for searching for their closest, but more complex structural analogues combining the properties noted above. From the point of view of atomic coordination, the closest candidates are crystals with the structure of chalcopyrite or antichalcopyrite, and in terms of composition, the most promising among beryllium binary compounds are crystals Be_3N_2, BeF_2, $BeCl_2$, $BeBr_2$ and BeI_2.

Beryllium dinitride Be_3N_2 is used in refractory ceramics and nuclear reactors [1], and two structural modifications have been experimentally established for it: cubic (α-Be_3N_2) [2,3] phase, stable under normal conditions, containing tetrahedra BeN_4 with common angles and edges, and hexagonal (β-Be_3N_2) a high-temperature phase obtained from the α-phase at temperatures above 1400°C [4] containing, in addition to the tetrahedra BeN_4, links BeN_3. Calculations for the hypothetical high pressure phase (γ-Be_3N_2), performed within the framework of the density functional theory by the method of linear combination of atomic orbitals [5], showed that γ-Be_3N_2 can be derived from α-Be_3N_2 and β-Be_3N_2 at very high pressures: 125 and 86 GPa, respectively.

Beryllium difluoride BeF_2 is used for the most efficient synthesis of beryllium metal [6], as well as in biochemistry as a phosphate simulator and, in an alloy with lithium fluoride, as a coolant in nuclear reactors. Anhydrous beryllium fluoride (BeF_2) has a much greater polymorphism [7] than Be_3N_2, it can crystallize in phases similar to silicon dioxide (SiO_2), including in the cristobalite structure (β-SiO_2), consisting of tetrahedra BeF_4 connected by vertices. Since the structure of β-SiO_2 is similar to the structure of chalcopyrite ($CuFeS_2$), consisting of three sublattices [8,9], where each atom is tetrahedrally surrounded by atoms of a different sort, you can choose crystals α-Be_3N_2 and BeF_2 as starting materials for modeling a triple diamond-like hypothetical compound: $Be_3N_2 + BeF_2 \rightarrow Be_2NF$. With the ordered filling of the corresponding sublattices, a Be_2NF crystal with the structure of antichalcopyrite [10] is obtained, in which the N and F atoms are placed in cationic sublattices, and the Be —atoms in anionic.

Beryllium dichloride $BeCl_2$ is used in medicine to diagnose tuberculosis, beryllium dibromide $BeBr_2$ in combination with diethyl ether is an extremely active catalyst for organic bromination reactions, and beryllium diiodide BeI_2 is used to produce high-purity beryllium [11].

The beryllium compounds discussed above have sufficiently similar characteristics, which allows us to consider them as a common basis for constructing an isocationic series of triple diamond-like hypothetical compounds Be_2NF, Be_2NCl, Be_2NBr and Be_2NI, and the purpose of this work is a theoretical study of the electronic and vibrational characteristics of these crystals based on the application of first-principle calculation methods.

2. Calculation method

Calculations of the electronic structure and dynamics of the lattice of crystals Be_2NA were performed within the framework of the density functional theory [12,13] in a local approximation to describe the effects of exchange and correlations [14] using the Quantum Espresso application package [15]. Two types of pseudopotentials were used to describe the electron-ion interaction: norm-preserving pseudopotentials with valence configuration $2s^2$ and $2s^22p^3$ were used for Be and N atoms; for anions F, Cl, Br, I — ultra-soft pseudopotentials [16] in the configuration ns^2np^5, $n = 2, 3, 4, 5$. To represent single-particle functions and electron density, the basis of plane waves with energies 100 Ry and 1000 Ry, respectively, was used; integration over the Brillouin zone was performed by the method of special points on the **k**-Monhorst-Pack grid [17] with dimension $4 \times 4 \times 4$. The complete optimization of the crystal geometry, including the lattice parameters and the positions of atoms in the cell, was performed using the quasi-Newtonian Broyden-Fletcher-Goldfarb-Shanno (BFGS) [18] method.

3. Results and discussion

The structure of the antichalcopyrite, Fig. 1, is the „inversion of the“ chalcopyrite structure — the spatial symmetry group I-42d — D_{2d}^{12} — № 122 [19] with by replacing anions in the formula ABC_2 with cations, i.e. A_2BC, subject to formal valence rules. The unit cell contains 8 atoms ($Z = 2$) located in positions with coordinates: Be — $(u, a/4, c/8)$, $(-u, -a/4, c/8)$, $(-a/4, u, -a/8)$, $(a/4, -u, -c/8)$; N — $(a/2, a/2, 0)$, $(a/2, 0, c/4)$, A — $(0, 0, 0)$, $(0, a/2, c/4)$. As an initial approximation, the ideal chalcopyrite structure was used to determine the structure of the crystals under study, for which the lattice parameters a and $c = 2a$ were determined using the values of the covalent radii of the corresponding atoms, and the value of $u = 0$ was set for the offset of cations. The results of geometry optimization are presented in Table 1.

As can be seen, the main parameters of the crystal structure of Be_2NA exhibit a characteristic series dependence, increasing with the increase in the atomic number of the halogen, and their changes correlate well with the corresponding changes in the atomic radii of halogens, which is expressed most noticeably during the transition from Be_2NF to Be_2NCl.

The band structure Be_2NA calculated for the most symmetric directions of the Brillouin zone, as well as the spectra of the total and projected density of states are shown in Fig. 2, where the vertex of the valence band is taken as the origin of the energy reference. Despite the differences in details that appear in the overall picture of the band structure when moving along a series of Be_2NA, the composition of atomic states indicates a significant similarity in the electronic structure of the crystals under consideration. At the same time, in the valence region, the full width of which varies in the range Be_2NA in the range from 24.0 to 16 eV, three groups of zones can be distinguished. The zones of the first group, located in the range from 0.0 to 8.0 eV, have a mixed character and are formed by p-states of nitrogen atoms with predominant contributions in the upper part, and p-states of halogen with the maximum contribution in the lower part; at the same time, for Be_2NF, a small gap is observed at energies of the order of -4.0 eV. The zones of the second group are located at a depth of about -12.0 eV and in composition almost completely correspond to the s-states of nitrogen atoms. The third group of zones is formed by s-states of halogen atoms, while their energies consistently increase from -24.0 to -12.0 eV, where in the case of Be_2NI, it merges with the zones s-nitrogen states whose position is practically unchanged.

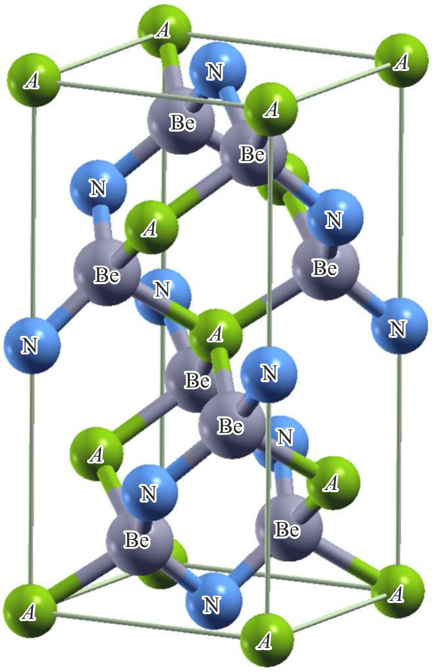

Figure 1. Crystal structure Be_2NA (A = F, Cl, Br, I).

Table 1. Crystal structure parameters Be_2NA

Be_2NA	a, Å	c, Å	c/a	u	Be–N, Å	Be–A, Å
Be_2NF	3.974	7.977	2.007	0.323	1.573	1.906
Be_2NCl	4.468	8.380	1.876	0.367	1.642	2.244
Be_2NBr	4.619	8.570	1.856	0.384	1.663	2.373
Be_2NI	4.811	8.938	1.858	0.408	1.700	2.560

All compounds Be_2NA, as follows from Fig. 2, are dielectrics with the band gap width 4.47 (Be_2NF), 3.33 (Be_2NCl), 2.73 (Be_2NBr) and 1.9 eV (Be_2NI). These values are underestimated due to a well-known feature of the local approximation of the density functional theory. To estimate more realistic values, a semi-empirical ratio can be used to

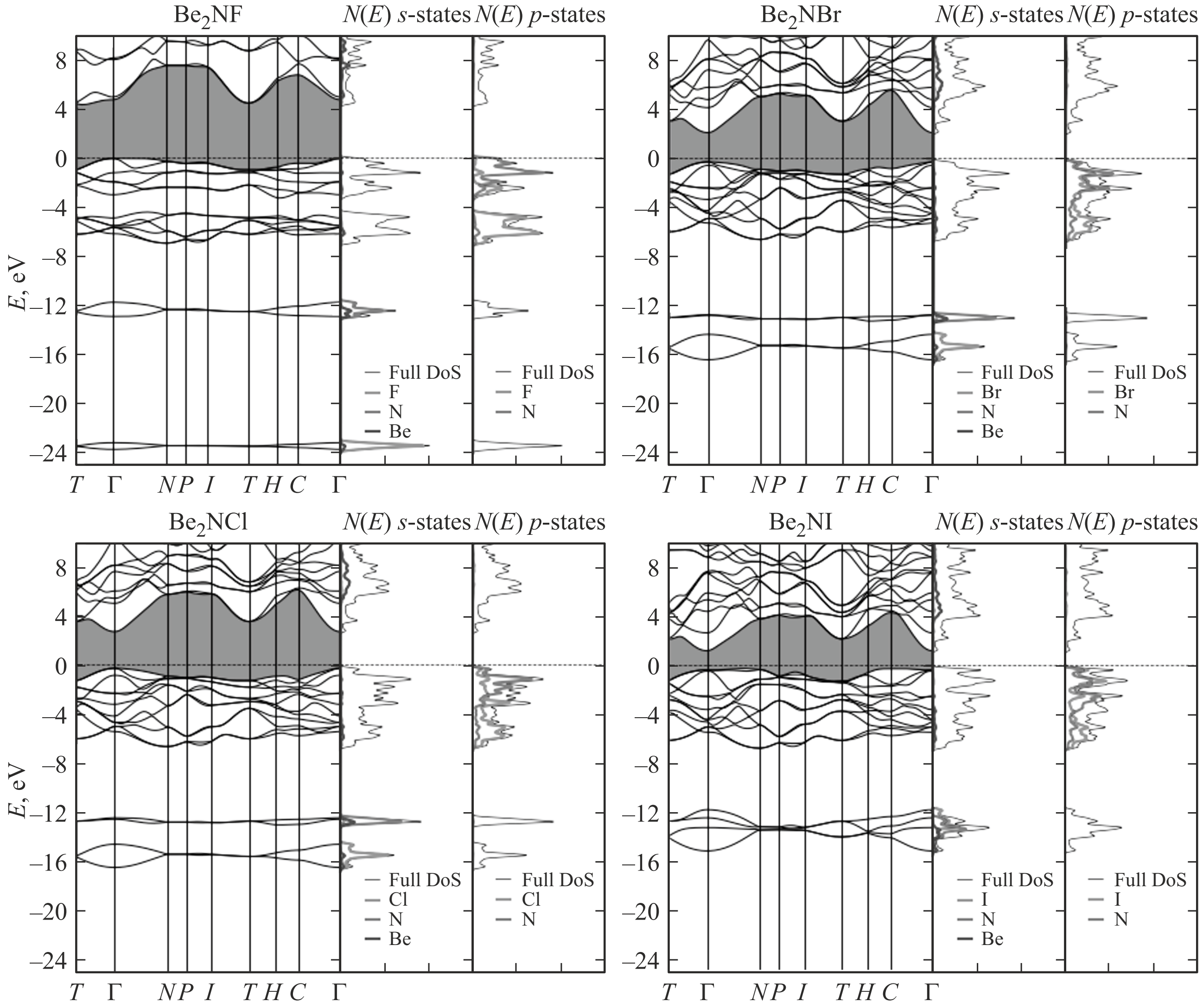

Figure 2. Zone structure, total and projected density of states Be_2NA (A = F, Cl, Br, I).

correct for the band gap width [20]:

$$\Delta_g, \text{eV} = \frac{9.3}{\varepsilon^{\infty}},$$

which, considering the results of Table 2, gives the values 7.23 (Be_2NF), 5.40 (Be_2NCl), 4.50 (Be_2NBr), 3.18 eV (Be_2NI).

Thus, it can be concluded that the zone structure is similar in basic features to the zone structure of crystals with the structure of (anti)chalcopyrite.

To analyze the type and features of the chemical bond in the compounds Be_2NA in this paper, maps of electron density distributions, Fig. 3, as well as electronic localization functions (ELF) are used [21–23], fig. 4. As can be seen from Fig. 3, all crystals are characterized by an almost complete absence of charge in the vicinity of beryllium atoms and a sufficiently strong localization of charge in the vicinity of nitrogen and halogen atoms, and for the latter it is maximal in the Be_2NF crystal. This indicates that all the compounds under consideration by the type of chemical bond are largely ionic. At the same time, when moving along the Be_2NA series, as a consequence of the increased hybridization of the p-states of nitrogen and halogens (Fig. 3), there is an increasingly noticeable tendency to generalize the charge between all three types of atoms, as indicated by the general contour covering them with a noticeable charge value, as well as a change in the shape of electronic clouds of nitrogen and halogen atoms, which become more elongated towards the atoms of beryllium.

The features noted above can also be observed on the maps ELF Be_2NA, Fig. 4, in which, in addition to the strong localization of electrons in the vicinity of nitrogen and halogen atoms, the presence of a covalent component of a chemical bond is manifested in the polarization of the ELF cloud of a nitrogen atom with the predominant localization on the N–Be line, as well as in the enhancement

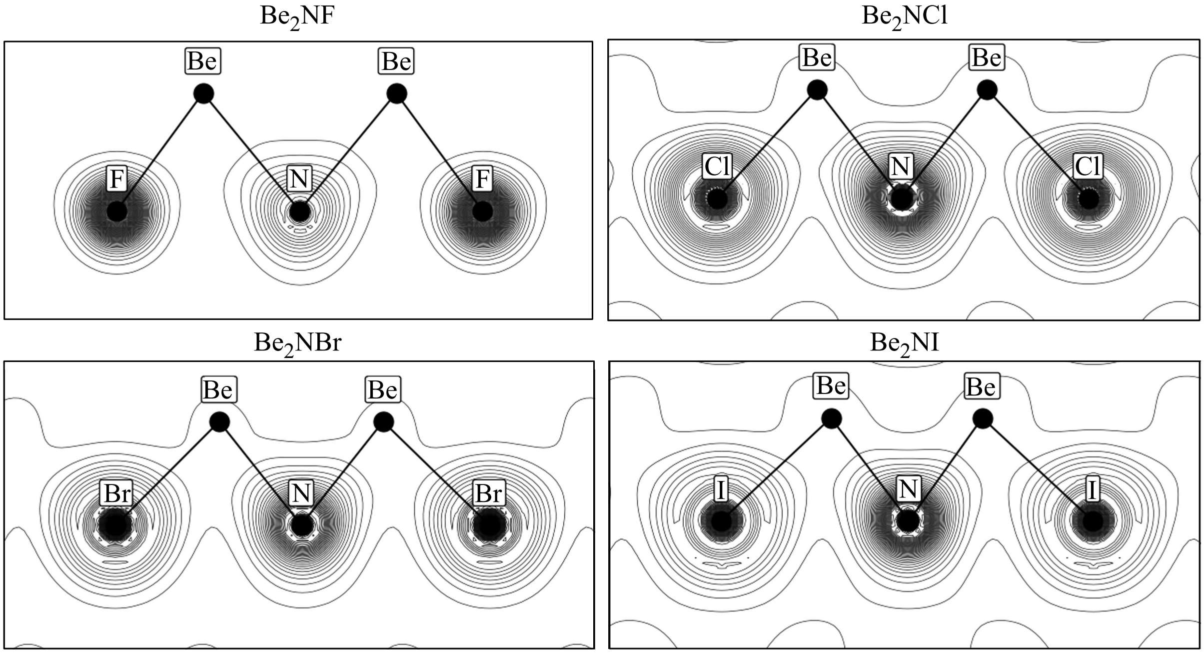

Figure 3. Total valence electron density in Be_2NA (A = F, Cl, Br, I).

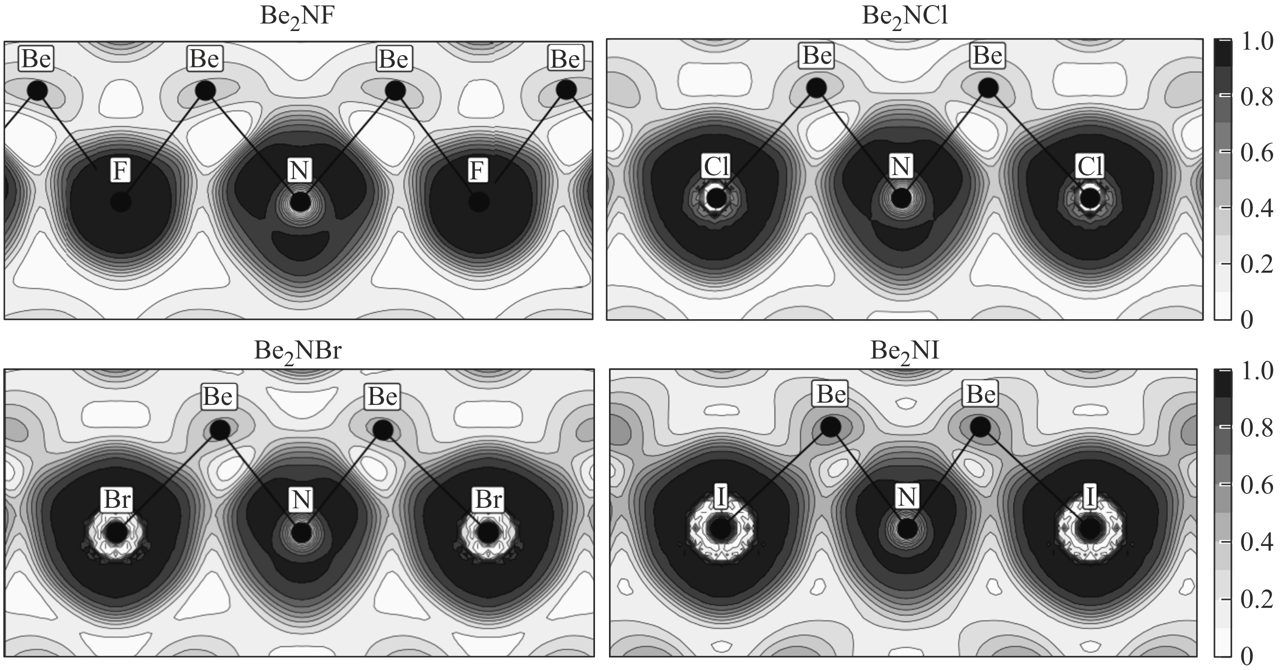

Figure 4. Electronic localization function (ELF) in Be_2NA (A = F, Cl, Br, I).

of the degree of localization of electrons on the Be$-A$ line, which in all cases exceeds the value of 0.25, characteristic of a homogeneous electron gas.

The results of calculating the response to an external, homogeneous electric field and collective offset of atoms performed for compounds Be_2NA include permittivity tensors, effective Born charges and phonon spectra.

In Table 2 and 3 represent the values of the main components of the permittivity tensors ($\varepsilon^{\infty,0}_{\parallel,\perp}$) and the effective Born charges, including the isotropic parts ($\varepsilon^{\infty,0} = (2\varepsilon^{\infty,0}_{\perp} + \varepsilon^{\infty,0}_{\parallel})/3$, $\langle Z_{\mathrm{atom}}\rangle = (\Sigma_i Z_{\mathrm{atom},ii})/3$).

As can be seen, the permittivity tensors differ in the degree of anisotropy, but have a general tendency to increase it in the series Be_2NA, which is consistent with an increase

Table 2. Dielectric constants of crystals Be_2NA

Be_2NA	$\varepsilon_{\perp}^{\infty}$	$\varepsilon_{\parallel}^{\infty}$	ε^{∞}	$\varepsilon_{\perp}^{0}$	$\varepsilon_{\parallel}^{0}$	ε^{0}
Be_2NF	3.44	3.24	3.37	13.41	5.38	10.74
Be_2NCl	4.63	4.19	4.48	13.80	6.10	11.23
Be_2NBr	5.46	4.80	5.24	15.16	6.75	12.36
Be_2NI	7.73	6.38	7.28	20.14	8.61	16.30

Table 3. Effective charge tensors Be_2NA (A = F, Cl, Br, I)

Z	Be_2NF	Be_2NCl	Be_2NBr	Be_2NI
$Z_{A,xx}$	−1.499	−1.450	−1.469	−1.580
$Z_{A,zz}$	−1.243	−0.934	−0.785	−0.512
$Z_{A,xy}$	−0.028	−0.033	−0.020	−0.071
$\langle Z_A \rangle$	−1.414	−1.278	−1.241	−1.223
$Z_{\mathrm{N},xx}$	−2.129	−2.610	−2.898	−3.441
$Z_{\mathrm{N},zz}$	−2.199	−2.479	−2.667	−3.018
$Z_{\mathrm{N},xy}$	−0.002	−0.123	−0.190	−0.283
$\langle Z_{\mathrm{N}} \rangle$	−2.152	−2.567	−2.812	−3.301
$Z_{\mathrm{Be},xx}$	1.794	2.133	2.372	2.846
$Z_{\mathrm{Be},yy}$	1.822	1.896	1.932	1.996
$Z_{\mathrm{Be},zz}$	1.729	1.710	1.730	1.760
$Z_{\mathrm{Be},yz}$	−0.160	0.018	0.077	0.149
$Z_{\mathrm{Be},zy}$	−0.230	−0.065	0.007	0.109
$\langle Z_{\mathrm{Be}} \rangle$	1.781	1.913	2.012	2.201

in the covalent nature of the bond, as already noted above. In relation to effective charges, the following features can be noted:

a) the degree of anisotropy increases with the transition from Be_2NF to Be_2NI and is the strongest for halogen atoms, for which the ratio of transverse (xx) and longitudinal (zz) components varies from 1.2 to 3.1, in contrast to the corresponding values of 0.97−1.14 for nitrogen atoms and 1.04−1.62 and beryllium;

b) the values of the effective charges in the series from Be_2NF to Be_2NI differ from the nominal ones, indicating, again, the presence of a covalent component of the chemical bond, but systematically approach them, which is most pronounced for the isotropic part of the tensors;

c) the presence of nonzero nondiagonal tensor components allows us to estimate the degree of spatial extent of the effective interaction with the crystalline environment, and for halogen atoms it is limited to the nearest neighbors, and for nitrogen and beryllium atoms we can talk about an increase in the influence of the second, etc. neighbors, and when changing the halogen from fluorine to chlorine, as follows from Table 3, the roles of these atoms are changing. The above features are determined by the electrochemical parameters of the atoms and correlate well with the values of electronegativity Be (1.6), N (3.0), F (4.0), Cl (3.0), Br (2.8), I (2.5), and in addition, allow consider Be_2NCl as a boundary connection in the series Be_2NA.

The vibrational spectrum of compounds Be_2NA contains 24 modes (8 atoms in an elementary cell). For the center of the Brillouin zone (point Γ), the complete vibrational representation can be decomposed by irreducible as

$$\Gamma_{\mathrm{vib}} = \mathrm{A}_1 + 2\mathrm{A}_2 + 3\mathrm{B}_1 + 4\mathrm{B}_2 + 7\mathrm{E},$$

at the same time, 3 modes of type (B_2 + 1 E) belong to acoustic, and the remaining 21 — to optical vibrations, which, with the exception of the hidden A_2-modes, are active in the infrared spectra (I: B_2, E) and Raman spectra (R: A_1, B_1, B_2, E). The oscillation frequencies at the point Γ are given in Table. 4, including splitting of longitudinal (LO) and transverse (TO) optical modes; at the same time, according to symmetry, oscillations of the type A_1 and A_2

Table 4. Oscillation spectrum Be_2NA (A = F, Cl, Br, I) in the center of the Brillouin zone (Γ) (cm^{-1})

Symmetry	Be_2NF	Be_2NCl	Be_2NBr	Be_2NI	Activity
A_1	657	510	460	379	R
A_2	985 645	581 860	822 563	751 521	
B_1	819 491 303	673 435 285	632 424 201	570 400 173	R
B_2 LO/TO	1183/1084 571/518 372/445	983/916 561/514 301/336	929/864 556/510 251/281	839/776 529/546 225/254	I+R
E LO/TO	932/993 700/771 484/513 355/336 329/284 230/261	782/846 593/647 460/497 285/282 265/276 242/245	736/807 551/563 441/482 270/270 239/242 177/177	658/739 490/487 414/454 275/276 228/224 147/147	I+R

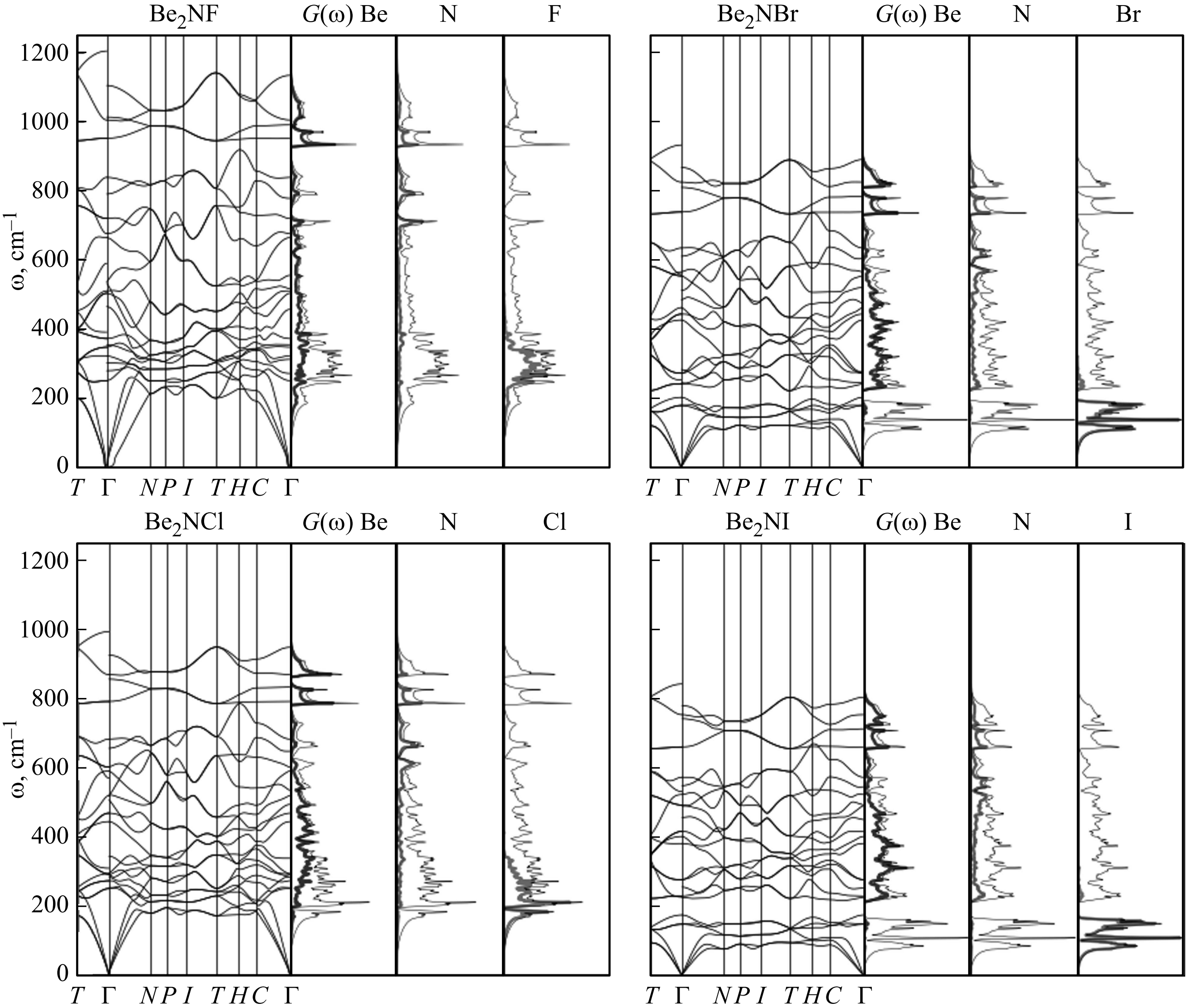

Figure 5. Phonon spectra Be$_2$NA (A = F, Cl, Br, I), total and projected frequency density (thin and bold lines, respectively).

are caused by the movement of only atoms of the cationic sublattice (contributions of Be atoms are 100%), and the rest are of a mixed nature.

The full phonon spectra of Be$_2$NA are shown in Fig. 5 and, in general, have a fairly general character, due to the crystal-chemical similarity of the compounds under consideration, and do not contain regions with imaginary frequencies, which indicates their stability. In all cases, the spectrum is divided into two well-defined regions: low-frequency in the range up to 200 cm^{-1}, where the oscillations are almost entirely due to the movement of the heavy sublattice of halogen atoms, and high-frequency, corresponding to the collective vibrations of the atoms of the light subsystem, whose contributions in the entire frequency range are competing. A relatively small transition region of the spectrum containing contributions of all three types of atoms is present for Be$_2$NF and Be$_2$NCl, but it shrinks very quickly and practically disappears for Be$_2$NBr and Be$_2$NI, in the spectrum of which, in addition, a gap appears. An increase in the mass of halogen atoms leads to a systematic decrease in the full width of the oscillation spectrum, which varies from ~ 1200 to ~ 850 cm^{-1}.

4. Conclusion

The first-principle calculations performed for the group of hypothetical crystals Be$_2$NA (A = F, Cl, Br, I) show that the crystals are stable in the structure of antichalcopyrite and are dielectrics whose band gap width decreases monotonically with the increase in atomic halogen numbers, up to values characteristic of semiconductors; and by the type of chemical bond Be$_2$NA should be attributed to strongly ionic compounds, but with a noticeable contribution of the covalent component. The above-mentioned features, as well as the analysis of a number of other characteristics, including dielectric constants, effective charges and parameters of vibrational spectra, thus allow us to classify the compounds considered as promising for the targeted synthesis of materials with specified properties.

Conflict of interest

The authors declare that they have no conflict of interest.

References

[1] H.O. Pierson. Handbook of Refractory Carbides and Nitrides: Properties, Characteristics, Processing, and Applications. William Andrew Inc., N.Y., USA (1996). 362 p.
[2] M. von Stackelberg, R. Paulus. Z. Phys. Chem. B **22**, *1*, 305 (1933).
[3] O. Reckeweg, C. Lind, A. Simon, F.J. DiSalvo. Z. Naturforschung **58**, *1*, 159 (2003).
[4] P. Eckerlin, A. Rabenau. Z. Anorg. Allg. Chem. **304**, *3–4*, 218 (1960).
[5] S.R. Römer, T. Dörfler, P. Kroll, W. Schnick. Phys. Status Solidi B **246**, *7*, 1604 (2009).
[6] A.F. Holleman, E. Wiberg, N. Wiberg. Inorganic Chemistry. Academic Press, San Diego, USA (2001). 1884 p.
[7] M.A. Zwijnenburg, F. Corá, R.G. Bell. J. Am. Chem. Soc. **130**, *33*, 11082 (2008).
[8] Yu.M. Basalaev, S.A. Marinova. Zhurn. strukturn. khimii **60**, *7*, 1067 (2019). (in Russian).
[9] Yu.M. Basalaev, A.S. Poplavnoi. Crystal chemistry, electronic and vibrational structure of compounds with chalcopyrite lattice. In: Chalcopyrite: Chemical Composition, Occurrence and Uses. Nova Science Publishers, Inc., N.Y., USA (2014).
[10] Yu.M. Basalaev, A.V. Sidorova. Izv. vuzov. Fizika **61**, *8*, 51 (2018).(in Russian).
[11] K.A. Bolshakov. Khimiya i tekhnologiya redkikh i rasseyannykh elementov (Chemistry and technology of rare and scattered elements). Vyssh. shk., M. (1976). V. 1. 368 p. (in Russian).
[12] P. Hohenberg, W. Kohn. Phys. Rev. **136**, *3B*, 864 (1964).
[13] W. Kohn, L.J. Sham. Phys. Rev. **140**, *4A*, 1133 (1965).
[14] J.P. Perdew, A. Zunger. Phys. Rev. B **23**, *10*, 5048 (1981).
[15] P. Giannozzi, S. Baroni, N. Bonini, M. Calandra, R. Car, C. Cavazzoni, D. Ceresoli, G.L. Chiarotti, M. Cococcioni, I. Dabo, A. Dal Corso, S. de Gironcoli, S. Fabris, G. Fratesi, R. Gebauer, U. Gerstmann, C. Gougoussis, A. Kokalj, M. Lazzeri, L. Martin-Samos, N. Marzari, F. Mauri, R. Mazzarello, S. Paolini, A. Pasquarello, L. Paulatto, C. Sbraccia, S. Scandolo, G. Sclauzero, A.P. Seitsonen, A. Smogunov, P. Umari, R.M. Wentzcovitch. J. Phys.: Condens. Matter **21**, *39*, 395502 (2009).
[16] D. Vanderbilt. Phys. Rev. B **41**, *11*, 7892(R) (1990).
[17] H.J. Monkhorst, J.D. Pack. Phys. Rev. B **13**, *12*, 5188 (1976).
[18] J. Nocedal, S.J. Wright. Numerical Optimization. Springer, USA (2006). 684 p.
[19] Yu.M. Basalaev. Elektronnoe stroenie troinykh almazopodobnykh soedineniy so strukturoi khal'kopirita: monografia (Electronic structure of triple diamond-like compounds with chalcopyrite structure: monograph). Kemerovo State University, Kemerovo (2009). 226 p. (in Russian).
[20] V. Fiorentini, A. Baldereschi. J. Phys.: Condens. Matter **4**, *27*, 5967 (1992).
[21] A.D. Becke, K.E. Edgecombe. J. Chem. Phys. **92**, *9*, 5397 (1990).
[22] A. Savin, O. Jepsen, J. Flad, O.K. Andersen, H. Preuss, H.G. von Schnering. Angew. Chem. Int. Ed. Engl. **31**, *2*, 187 (1992).
[23] A. Savin, R. Nesper, S. Wengert, T.F. Fässler. Angew. Chem. Int. Ed. Engl. **36**, *17*, 1808 (1997).